Metabolic profiling following immunological perturbations: comparison across individuals from different geographical areas

Betouke Ongwe, M.E.

Chapter 5

Potentiation of the axis involving pentose phosphate pathway/NADPH oxidase/ reactive oxygen species drives higher IL-10 production in monocytes of Sub-Saharan Africans

Madeleine Eunice Betouke Ongwe[1-3], Yoanne D. Mouwenda[1,2], Mikhael D. Manurung[1], Graham Heieis[1], Shohreh Azimi[1], Ayola A. Adegnika[1,2,4,5], Peter G. Kremsner[2,4], Taco W. Kuijpers[6,7], Maria Yazdanbakhsh[1*] and Bart Everts[1*]

1 Leiden University Center of Infectious Diseases, Leiden University Medical Center, Leiden, The Netherlands.
2 Centre de Recherches Médicales de Lambaréné, Lambaréné, Gabon.
3 Institut de Recherches en Écologie Tropicale, Centre National de la Recherche Scientifique et Technologique, Libreville, Gabon
4 Institut für Tropenmedizin, Eberhard-Karls-Universität Tübingen, Germany.
5 German Center for Infection Research, Tübingen, Germany.
6 Sanquin Research, and Landsteiner Laboratory, Academic Medical Center, University of Amsterdam, Amsterdam, The Netherlands.
7 Emma Children's Hospital, Academic Medical Center, Dept of Paediatric Immunology, Rheumatology and Infectious Diseases, University of Amsterdam, Amsterdam, The Netherlands.
M.Y. and B.E. contributed equally.
* Corresponding authors: Bart Everts, e-mail: b.everts@lumc.nl; and Maria Yazdanbakhsh E-mail : m.yazdanbakhsh@lumc.nl. Leiden University Center of Infectious diseases, Albinusdreef 2, 2333 ZA Leiden, The Netherlands.

Eur J Immunol. 2024 Jun 14:e2451029.
PMID: 38873882.
doi: 10.1002/eji.202451029

ABSTRACT

Cellular metabolism is a key determinant of immune cell function. Here we found that CD14+ monocytes from Sub-Saharan Africans produce higher levels of IL-10 following TLR-4 stimulation and are bioenergetically distinct from monocytes from Europeans. Through metabolomic profiling, we identified the higher IL-10 production to be driven by increased baseline production of NADPH oxidase-dependent reactive oxygen species, supported by enhanced pentose phosphate pathway activity. Together, these data indicate that NADPH oxidase-derived ROS is a metabolic checkpoint in monocytes that governs their inflammatory profile and uncovers a metabolic basis for immunological differences across geographically distinct populations.

Keywords

monocytes, ROS, pentose phosphate pathway, NADPH-oxidase, IL-10.

INTRODUCTION

Adaptation of immune responses that are known to vary between human populations from different geographical regions are driven by both genetic and environmental factors [1, 2]. Among the immune cell populations that have been shown to be functionally different between populations are monocytes, as evidenced by altered baseline activation marker expression and subset distribution [3], TLR responsiveness [4] and susceptibility to viral infection [5]. Monocytes are central players in the immune response by contributing to the initiation and resolution of inflammation [6]. Monocytes can be attracted by various signals including those derived from pathogens and commensals, and can traffic to the site of inflammation, and produce both inflammatory and anti-inflammatory cytokines to shape local and systemic inflammatory responses [7, 8]. Mapping molecular features that underlie the inflammatory profiles of monocytes, may help identifying novel pathways that can be targeted to modulate their function to treat disease.

There is a growing appreciation that monocyte activation, pro and anti-inflammatory cytokine production and induction of trained immunity, are associated with, and dependent on, rewiring of cellular metabolic pathways [9-12]. Here, we characterized the immunometabolic phenotype of monocytes of healthy adults from Europeans and Sub-Saharan Africans living in the Netherlands and Gabon, respectively, two populations we previously described to have distinct immune profiles [13]. We found clear differences in the core metabolic pathways between $CD14^+$ monocytes from the two groups. Immunological and in-depth metabolic characterization of the monocytes revealed that monocytes from African donors produced higher levels of the anti-inflammatory cytokine IL-10 upon TLR4 stimulation and had higher baseline NAPDH-oxidase activity. Furthermore, we identified elevated NADPH oxidase-derived ROS, fuelled by increased pentose phosphate pathway activity, as the main driver of the enhanced IL-10 production by monocytes from Africans. These findings establish a novel functional link between immunometabolic differences and anti-inflammatory profiles of monocytes, and as such provides important new insights in the molecular mechanisms underlying the differences in inflammatory immune profiles observed between populations from Europe and Sub-Saharan Africa.

RESULTS

Within PBMCs from Africans and Europeans, monocytes show greatest divergence in metabolism

To explore whether there are baseline metabolic differences in CD14$^+$ monocytes between Africans and Europeans, we analysed the core metabolic pathway activity in unstimulated CD14$^+$ monocytes isolated from PBMCs from healthy Gabonese and Dutch adults, respectively (the main study population characteristics can be found in Table S1), using real time extracellular flux analysis (Figure 1A). Monocytes from Europeans were found to have significantly higher oxygen consumption rates (OCR), as a measure for mitochondrial oxidative phosphorylation (OXPHOS), compared to Africans, both in terms of baseline and ATP-coupled respiration, spare respiratory capacity and maximum mitochondrial respiration (Figure 1B), indicating overall higher mitochondrial respiratory activity. In contrast, no significant differences were observed in extracellular acidification rate (ECAR) as a measure of glycolysis, between the two groups (Figure 1C). Of note, the bioenergetic differences in total PBMCs between the two groups (Figure 1D and S1), were mirrored by the bioenergetic profiles of the monocytes, with a similarly higher baseline respiration in Europeans compared to Africans but with no significant difference in glycolytic parameters (Figure 1E). This suggests that within the PBMCs of Africans and Europeans, the monocytes display the most profound bioenergetics differences and that the metabolic differences observed in the PBMCs as a whole, are a direct reflection of differences in monocyte metabolism (Figure S2). Of note, this is not a consequence of higher frequencies of CD14$^+$ monocytes in Africans, as these cells were present at lower frequencies in PBMCs from Africans compared to Europeans (Figure S3).

We next assessed whether these differences in core metabolism were associated with an altered functional profile in isolated monocytes. Upon stimulation with TLR4 ligand LPS, CD14$^+$ monocytes from African donors, produced significantly higher levels of anti-inflammatory IL-10 compared to those from Europeans, while the opposite was true for pro-inflammatory cytokine TNF (Figure 1F). Within each cohort there was no difference in IL-10 production between male and female, nor was it affected by age (data not shown). No differential expression of pro-inflammatory cytokines IL-1b or IL-6 was observed (Figure 1F). This suggests that monocytes from Africans are both metabolically and functionally distinct from those of Europeans, characterized by a more anti-inflammatory profile.

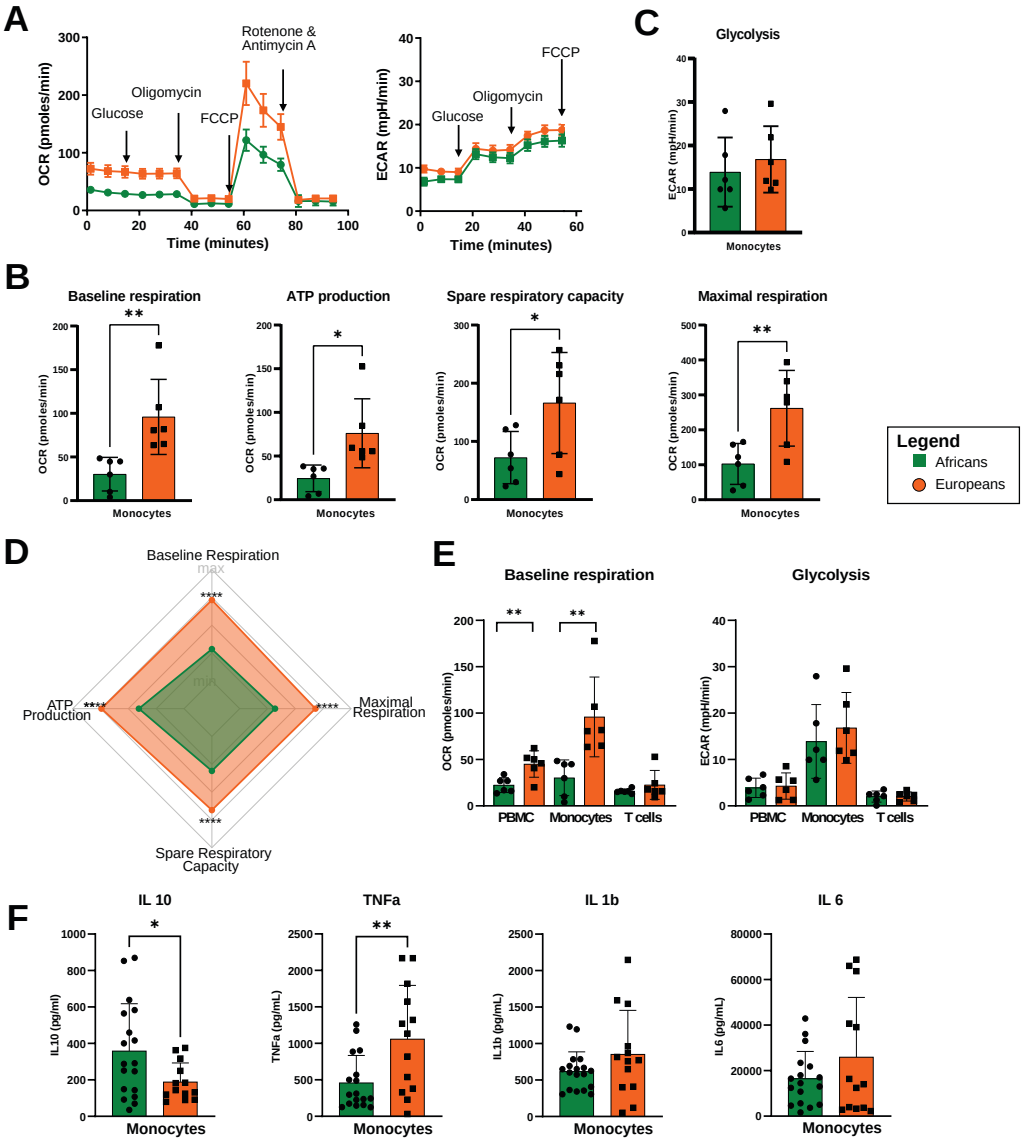

Figure 1. Monocytes from Africans have a distinct bioenergetic and cytokine profile compared to monocytes from Europeans. (A) Oxygen consumption rate (OCR) and extracellular acidification rate (ECAR) were determined in live CD14+ monocytes of Europeans and Africans using the seahorse XF analyser. A representative plot of a glucose and mitochondrial stress test. (B) Based on mitochondrial stress test, baseline respiration, ATP production, spare respiratory capacity and maximal mitochondrial respiration was determined in monocytes. C) Based on glycolysis stress test baseline, glycolytic rates of CD14+ monocytes were determined (D) Based on mitochondrial stress test, baseline respiration, ATP production, spare respiratory capacity and maximal mitochondrial respiration was determined in PBMCs. (E) Baseline respiration (OCR) and glycolysis (ECAR) of CD14+ monocytes and CD4+ T cells isolated from total PBMCs. (F) IL-10, TNFα, IL-1β, IL-6 production by monocytes of Europeans and Africans after LPS stimulation as determined by ELISA in culture supernatants. Bars represent mean ± SD; each dot represents one individual. *, P < 0.05, **,P < 0.01, ***P < 0.001, ****P < 0.0001 for significant differences between Europeans and Africans based on unpaired Student's T test.

Monocytes from Africans display reduced mitochondrial metabolism compared to Europeans

To start addressing whether the differences in monocyte metabolism between Africans and Europeans could explain the divergence in their inflammatory profile, we performed a more in-depth metabolic characterisation and comparison of the $CD14^+$ monocytes from both groups. Flow cytometry-based analysis of mitochondrial membrane potential and mass revealed no differences in the former, but a higher signal of the latter in monocytes from Africans, which may indicate that the lower OXPHOS in monocytes from Africans is a reflection of reduced activity, rather than being a consequence of reduced mitochondrial content (Figure 2A). Additionally, higher mitochondrial mass was not a consequence of increased cell size because that was comparable for monocytes from Africans and Europeans as determined by forward-scatter width (FSC-W) (Figure 2B).

Indeed, spectral flow cytometry-based analysis of protein expression of mitochondrial electron transport chain complexes, Succinate dehydrogenase A (SDHA) and cytochrome C (CytC) [14, 15], showed no reduced expression in African monocytes (Figure 2C). On the other hand, we did observe reduced expression of Carnitine Palmitoyltransferase (CPT1a), a rate limiting transporter required for mitochondrial long chain fatty acid oxidation (FAO), in African monocytes (Figure 2C), hinting towards lower FAO, which could in part explain the reduced OXPHOS in these cells. Consistent with comparable glycolytic rates (Figure 1C and D), uptake of fluorescent glucose analog 2NBDG by monocytes, was not different between the groups (Figure 2D), nor was there a difference in expression of rate limiting enzyme in glycolysis, Pyruvate Kinase (PKM), or glucose transporter (Glut1) (Figure 2D).

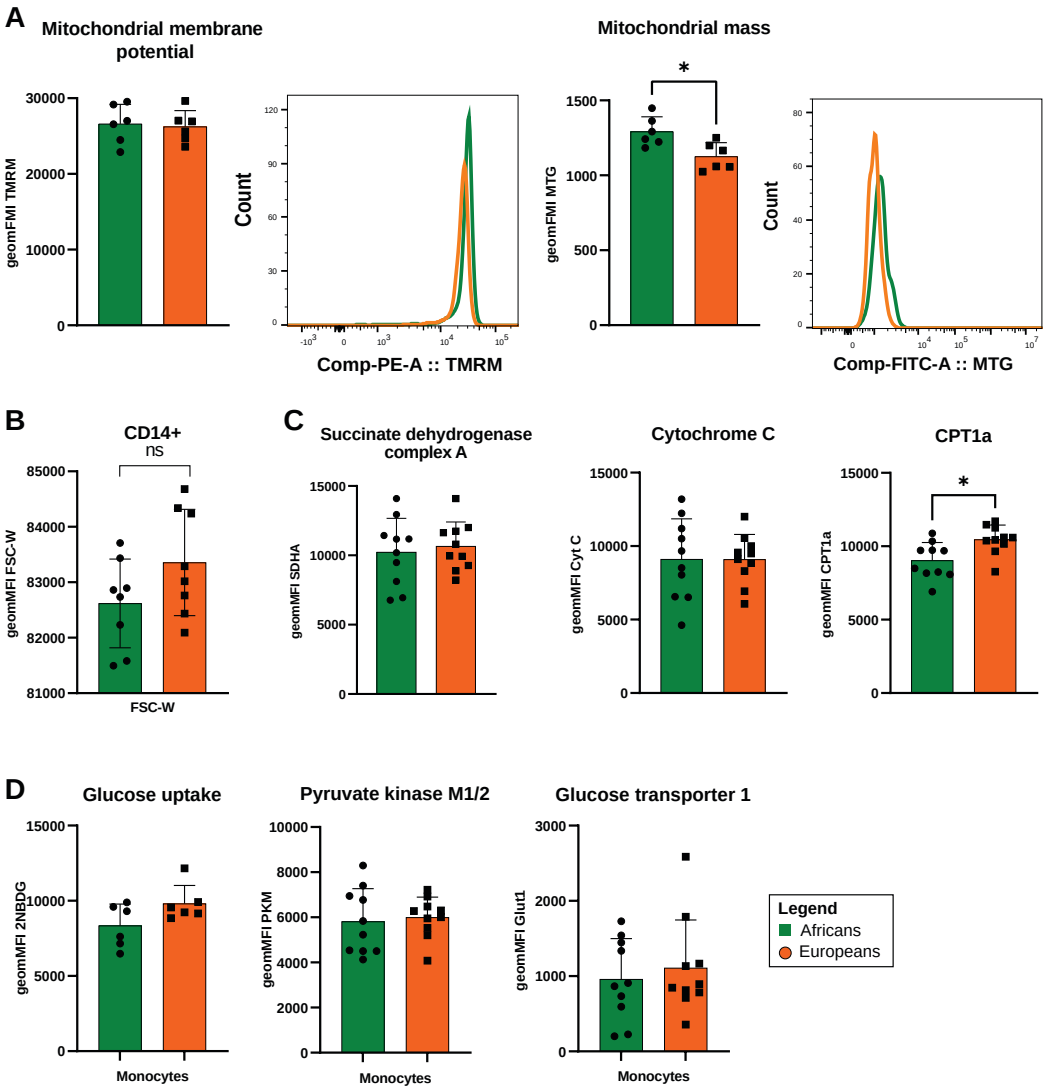

Figure 2. Monocytes from Africans display reduced mitochondrial metabolism at steady state. (A) Geometric mean fluorescence (geomMFI) of Tetramethyl rhodamine (TMRM) and MitoTracker green (MTG), parameters of mitochondrial membrane potential and mitochondrial mass, respectively, were recorded for isolated CD14+ monocytes from Europeans and Africans using flow cytometry. The histogram shows one representative example of the TMRM and MTG staining. (B) Monocytes size of Europeans and Africans measured by the mean of forward scatter width (FSC-W). (C) GeomMFI of succinate dehydrogenase A (SDHA) and cytochrome C (CytC), Carnitine Palmitoyltransferase (CPT1a); and (D) Pyruvate Kinase 1/2 (PKM) and glucose transporter (Glut1) of Europeans and Africans determined by spectral flow cytometry. Bars represent mean ± SD; each dot represents one individual. *, P < 0.05, for significant differences between Europeans and Africans based on unpaired Student's T test.

To further expand these findings, quantitative untargeted metabolomics was performed on monocytes from both groups. A differential analysis showed that 178 out of 277 annotated metabolites were significantly different between Africans and Europeans (Table S1). Among them, 93 metabolites were upregulated in Europeans whereas 85 metabolites were upregulated in Africans (Figure 3A).

Unsupervised clustering analysis of these metabolites revealed distinct clustering patterns among African and European donors. This differentiation was primarily attributed to two sets of clusters representing metabolite abundances in monocytes from the respective study groups. Cluster 1 exhibited metabolites that were more abundant in Europeans, while cluster 2 consisted of metabolites that were more abundant in Africans. (Figure 3B). Several metabolic pathways were significantly enriched in cluster 1, in particular those related to amino acids such as alanine, arginine, glutamine and valine (Figure 3C, D). In addition, cluster 1 was also significantly enriched for TCA cycle metabolites including acetyl-CoA, itaconate, succinate, fumarate, and malate (Figure 3C-E). Conversely, tyrosine metabolism was the only metabolic pathway significantly enriched in Cluster 2 (Figure 3C). This corresponded with a higher concentration of dopamine, of which tyrosine is the precursor, in monocytes from Africans (Figure 3F).

Unbiased metabolic network topology analysis based on differential abundance of total metabolites, confirmed reduced TCA cycle metabolites and increased tyrosine metabolism as key metabolic features discriminating African from European monocytes (Figure 3E). Difference in abundance of metabolites linked to glycolysis were less uniform (Figure 3D). While glucose and lactate levels were significantly higher in Europeans, the opposite was true for glucose/fructose-6P suggesting a possibly enhanced diversion of carbons from glycolysis into an ancillary pathway such as the pentose phosphate pathway (PPP) in monocytes from Africans. However due to technical limitations, PPP intermediates could not be detected to substantiate this idea.

Overall, these data suggest that ex vivo monocytes from Africans are metabolically distinct from their European counterparts, with lower activity in mitochondrial TCA cycle and respiration as well as in overall amino acid metabolism, but with upregulation of tyrosine metabolism as a notable exception, while overall glycolytic rates appear not to significantly differ.

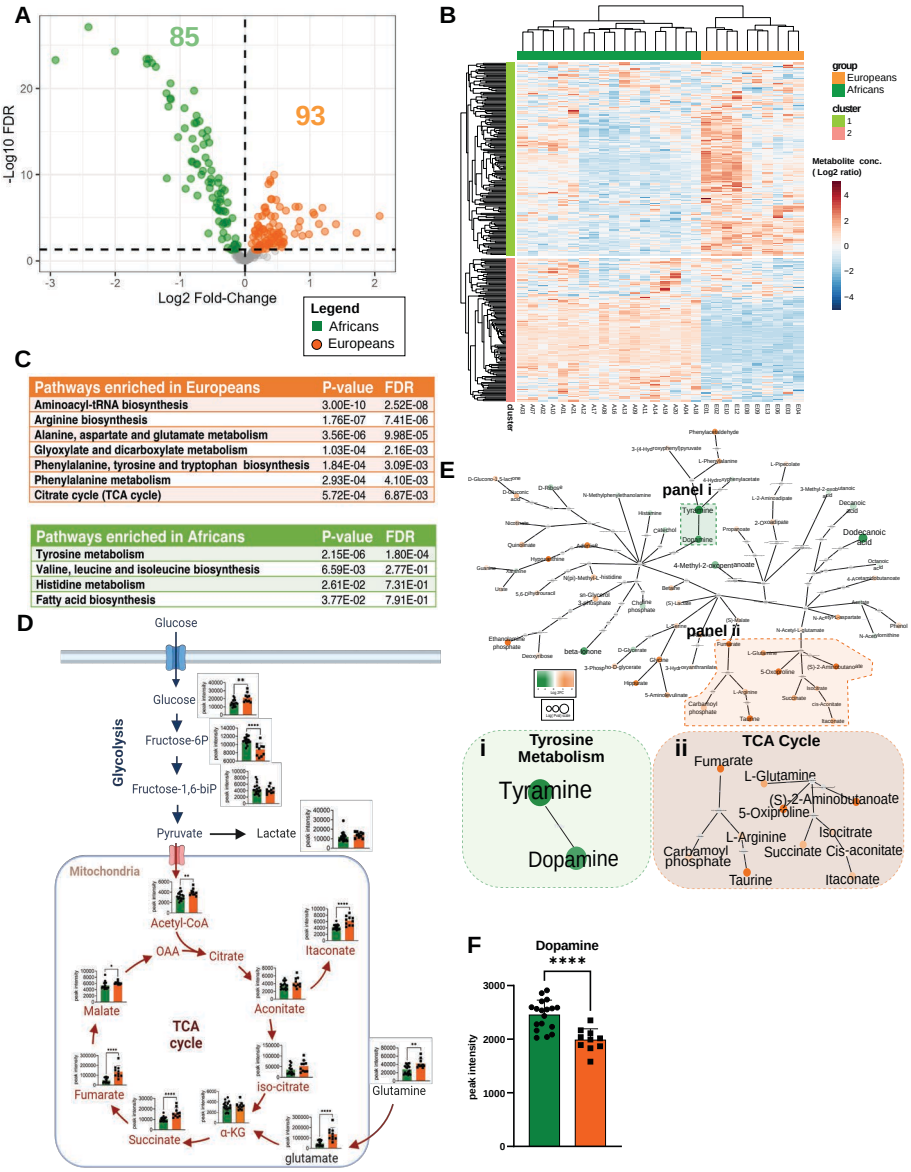

Figure 3. Untargeted metabolomics reveals differential metabolite network enrichment in monocytes from Africans and Europeans . Quantitative LC-MS-based metabolomics was performed on monocyte lysates from Africans and Europeans. (A) A volcano plot of 277 metabolites in which green and orange metabolites indicate the ones that are significantly upregulated in Africans (n=85) or in Europeans (n=93), respectively. P-values were corrected for false discovery rate (FDR) and the FDR is set at 0.05 level. (B) A heatmap representing an unsupervised clustering analysis of differentially abundant metabolites (rows) from panel (a) comparing Africans and Europeans subjects (columns). Color of the heatmap tiles represent log2 ratio of metabolite concentration (Conc.) between Africans and Europeans.(C) Tables of the top pathways enriched in Africans and Europeans. Metabolites with HMDB identification number (HMDB ID) that are

upregulated in Africans (cluster 2) and in Europeans (cluster 1) described in Figure 3b that were loaded in MetaboAnalyst 5.0. (D) Metabolite levels (ion mean intensity) within indicated core metabolic pathway. (E) Metabolic network topology of metabolites with differential abundance in monocytes from Africans and Europeans in which p-value (log(Pval) scale) and log2 fold change (log2FC) of metabolites are indicated. (F) Level of dopamine in monocyte lysates from Africans and Europeans. Bars represent mean ± SD; each dot represents one individual. *, P < 0.05, **,P < 0.01, ***P < 0.001, ****P < 0.0001 for significant differences between Europeans and Africans based on unpaired Student's T test.

NADPH oxidase-derived ROS fueled by the pentose phosphate pathway underpins enhanced IL-10 production in monocytes from Africans

In myeloid cells, ROS, in particular those generated in the mitochondria, have been shown to be an important regulator of IL-10 expression upon TLR stimulation [16]. This prompted us to assess ROS levels in the monocytes from both groups. Whereas no differences were found in steady state mitochondrial ROS production by monocytes between Africans and Europeans (Figure 4A), assessment of total cellular ROS levels at baseline revealed a significantly higher abundance in African monocytes compared to those from Europeans, which was retained following LPS stimulation (Figure 4B). Next, to assess the functional relevance of these findings, we used the ROS scavengers, N-acetyl-cysteine (NAC) and mitoquinone (MQ), to neutralize total or mitochondrial ROS, respectively. Importantly, pre-treatment with NAC resulted in a profound decrease in LPS-induced IL-10 production by monocytes from Africans, while MQ had only a modest effect. In contrast, none of these effects were observed in monocytes from Europeans (Figure 4C). This points towards a key role for non-mitochondrial ROS in promoting increased IL-10 production in monocytes from Africans.

A main source of non-mitochondrial ROS in myeloid cells is NADPH oxidase which uses NADPH and oxygen as substrates to generate ROS [17]. We found a higher expression of a subunit of NADPH oxidase, NOX2, in monocytes from Africans (Figure 4D). Moreover, when monocytes were treated with a NADPH oxidase inhibitor, diphenyleneiodonium chloride (DPI), we found a significant reduction of total ROS levels. In contrast, total ROS levels were unaffected by antimycin A plus rotenone treatment, that inhibit mitochondrial ROS production originating from Complex III and I from the electron transport chain (ETC) (Figure 4E), strongly suggesting that NADPH oxidase is the main source of increased total ROS levels in these cells. Indeed, inhibition of NADPH oxidase with DPI strongly decreased IL-10 production by monocytes from Africans and much less so by those from Europeans (Figure 4F). This effect appeared to be specific for IL-10 in monocytes from Africans, as TNF production by these cells was not affected by NADPH oxidase inhibition in Africans (Figure S5).

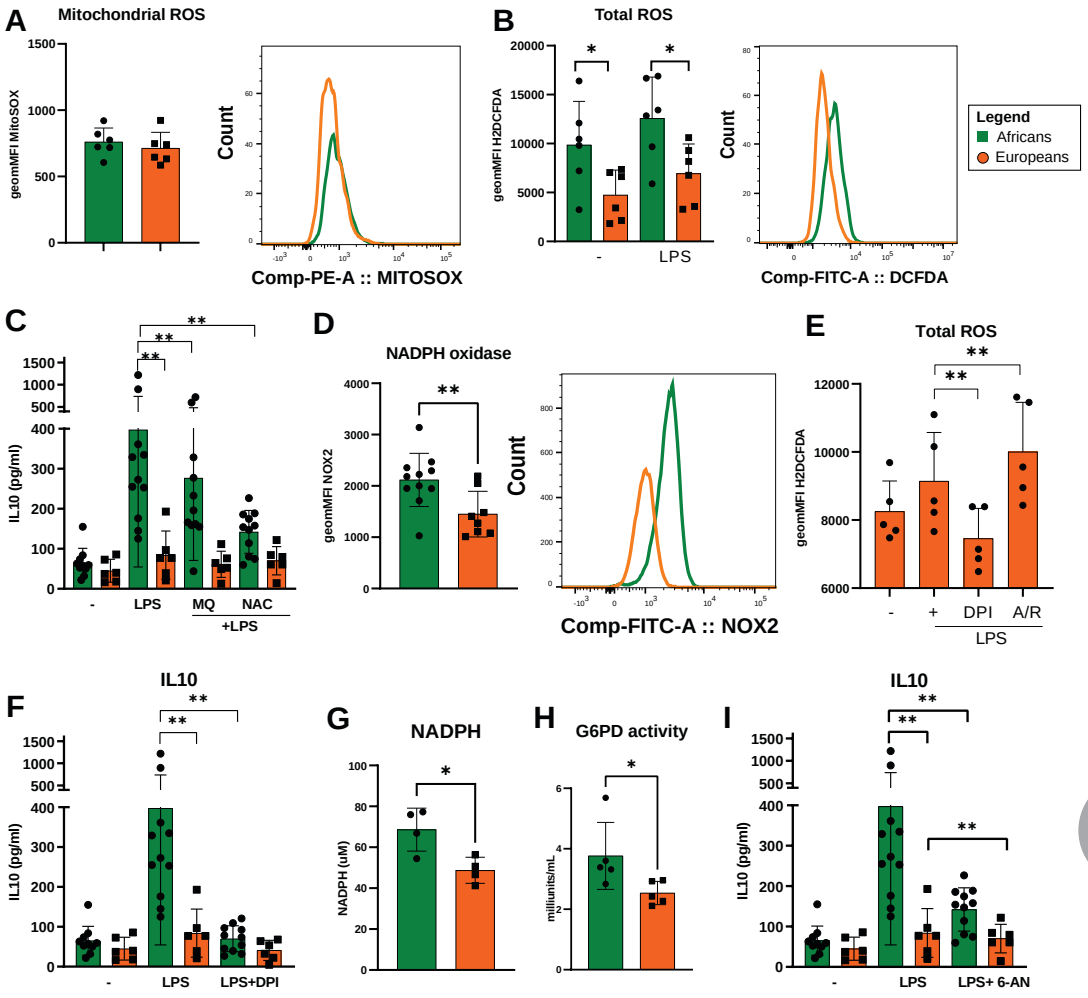

Figure 4. NADPH oxidase-derived ROS fueled by PPP underpins IL-10 production by monocytes from Africans. (A) Level of mitochondrial ROS measured in CD14+ monocytes of Africans and Europeans at steady state by flow cytometry using the MitoSOX dye. The histogram shows one representative example of MitoSOX staining. (B) Level of Total ROS measured by flow cytometry using H2DCFDA in monocytes of both groups at steady state after LPS stimulation. Histogram shows one representative example of H2DCFDA staining at steady state in Africans and Europeans. (C) IL-10 production after LPS stimulation in both groups in presence or absence of mitochondrial ROS scavenger (MQ) and cytoplasmic ROS scavenger (NAC). (D) NADPH oxidase 2 (NOX2) expression measured by flow cytometry for both groups at steady state. Histogram is one representative example of NOX2 staining. (E) Level of total ROS with and without a pre-treatment with NAPDH oxidase inhibitor (DPI) or inhibitors of mitochondrial ROS, antimycin A and rotenone (A/R). (F) IL-10 production after LPS stimulation in both groups with or without a pre-treatment with DPI.(G) Measurement of NADPH concentration and (H) G6PD activity at steady state in monocytes of both groups. (I) IL-10 production in presence or absence of pentose phosphate pathway inhibitor (6-AN). Bars represent mean ± SD; each dot represents one individual. *, P < 0.05, **,P<0.01, ***P<0.001, ****P<0.0001 for significant differences between Europeans and Africans based on unpaired Student's T test. DPI: diphenyleneiodonium; A/R: antimycin A / rotenone; MQ: mitoquinone; NAC:N-acetyl-cysteine.

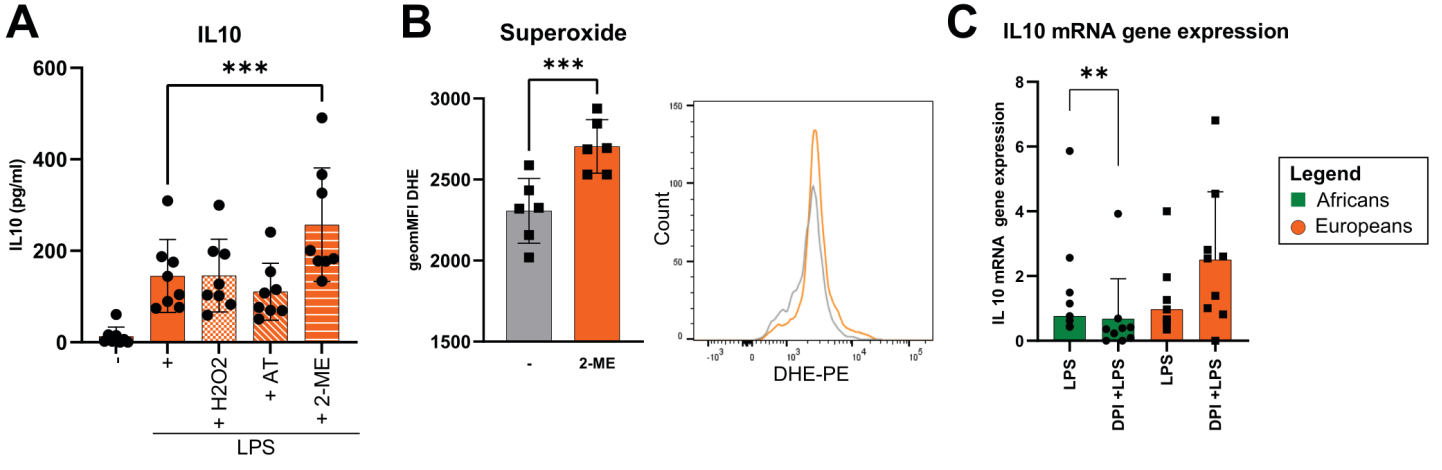

Figure 5. NADPH oxidase-derived superoxide boosts IL-10 production in Europeans and regulates IL-10 transcriptionally. (A) IL-10 production by European monocytes following LPS stimulation in the presence of ROS generators, 2-ME, AT and H2O2. (B) Superoxide production in European monocytes in absence (in grey) and in presence (in orange) of 2-methoxyestradiol (2-ME) treatment as determined by flow cytometry using dihydroethidium (DHE), a superoxide dye. Histogram shows one representative example of DHE staining. (C) IL-10 mRNA gene expression in LPS-stimulated monocytes in presence or absence of DPI in Africans and Europeans. Bars represent mean ± SD; each dot represents value of one individual. Paired Student's T test was performed to assess significant differences within Europeans or Africans group. **,P < 0.01, ***P < 0.001. DPI: diphenyleneiodonium; 2-ME: 2-methoxyestradiol; AT: 3-amino-2,3,4-triazole.

The oxidative branch of the PPP, malic enzyme 1 (ME1) and isocitrate dehydrogenase 1 (IDH1) are considered three main cellular sources of NADPH, of which particularly the former has been linked to supplying this substrate for NADPH oxidase [18]. In line with this, NADPH levels (Figure 4G) as well as enzymatic activity of glucose-6-phosphate dehydrogenase (G6PD), a rate-limiting enzyme of the PPP (Figure 4H), was significantly higher in monocytes from Africans compared to Europeans. Finally, we assessed the functional relevance of this increased PPP activity in regulating IL-10 production by monocytes, and we found that 6-aminonicotinamide (6-AN), an inhibitor of the pentose phosphate pathway (PPP), significantly decreased IL-10 production following LPS stimulation in both groups, with the strongest effects on the African monocytes (Figure 4I). Together, these findings identify ROS derived from enhanced NADPH-oxidase activity, fuelled by the PPP in African monocytes as the mechanism that underlies their potentiated IL-10-producing capacity.

NADPH oxidase-derived superoxide underpins IL-10 production in monocytes from Africans by controlling transcription

To further verify that ROS promotes IL-10 in monocytes from Africans, we tested whether boosting accumulation of ROS would be sufficient to enhance IL-10 production and if so which particular types of ROS would be required for that. NADPH-oxidase produces superoxide, which is converted by superoxide dismutase (SOD) into hydrogen peroxide (H_2O_2), that in turn is further detoxified into H_20 by catalase. While monocytes from Europeans did not display enhanced LPS-induced IL-10 production following exposure to H_2O_2 or a catalase inhibitor (AT, 3-amino-2,3,4-triazole) to promote accumulation of endogenous H_2O_2, they did following treatment with SOD1 inhibitor, 2-methoxyestradiol (2-ME) (Figure 5A) which enhanced superoxide accumulation (Figure 5B). This indicated that only the short-lived and highly reactive NADPH oxidase-derived superoxide, but not other ROS such as hydrogen peroxide accumulation, is promoting IL-10 production by monocytes.

Finally, we aimed to determine how ROS controls IL-10 expression. Given the known role for ROS in regulating the function of several transcription factors, such as NF-kB that downstream of TLR4 signalling controls IL-10 expression [19, 20], we hypothesized that NADPH oxidase-derived ROS affects IL-10 expression at the transcriptional level. We found that LPS-induced IL-10 mRNA expression was significantly decreased in the presence of DPI in Africans but not in Europeans (Figure 5C), indicating that NADPH oxidase activity regulates IL-10

expression transcriptionally in monocytes from Africans. Together, these data suggest the enhanced ability of monocytes from Africans to produce IL-10 following TLR stimulation is dependent on NADPH oxidase derived superoxide by acting on transcription.

DISCUSSION

Here we have found that that monocyte of Africans living in Gabon, produced higher levels of IL-10, an anti-inflammatory cytokine, upon TLR4 stimulation, compared to Europeans. They have higher baseline NADPH oxidase activity and we provide evidence that elevated NADPH oxidase-derived ROS is the main driver of the higher IL-10 production by monocytes from Africans.

An in-depth metabolic comparison of monocytes isolated from Africans and Europeans, revealed striking differences in their metabolic profile at baseline. First, we found that at steady state, monocytes from Africans display reduced OXPHOS despite having no apparent defects in electron transport chain (ETC) protein expression, or loss of mitochondrial mass. Furthermore, these cells displayed lower concentrations of TCA cycle substrates and intermediates, suggesting an overall decrease in mitochondrial activity. Interestingly, this was not mirrored by an increase in glycolysis, indicating that these cells have reduced ATP turnover and are more bioenergetically quiescent compared to Europeans counterparts. Indeed, a significant decrease in aminoacyl-tRNA biosynthesis, a crucial step in protein synthesis and one of the most energy-consuming processes in cells [21], was lower in the monocytes of Africans, while Europeans showed a significant enrichment in this process (Figure 3C). However, the causal relationship and potential immunological implications of these findings remain to be determined. Among the TCA intermediates that were present at higher concentrations in monocytes from Europeans than from Africans were succinate and α-ketoglutarate, two metabolites that have been shown to have the potential to affect the balance in pro- and anti-inflammatory cytokine production by myeloid cells. Succinate can promote IL-1β expression following TLR stimulation by supporting HIF-1α stabilization [22]. However, we did not find differences in IL-1β expression between the two groups, suggesting that IL-1β expression following TLR stimulation in monocytes is not affected by differences in baseline succinate levels. α-ketoglutarate can epigenetically promote the expression of anti-inflammatory genes, including IL-10 [23] by regulating activity of Jumonji C domain-containing histone demethylases (JmjC) [24]. However, given that we found high IL-10 expressing

African monocytes to have comparable α-ketoglutarate levels to Europeans, it is unlikely that the differential abundance of α-ketoglutarate between the two groups is an important driver of the differences in IL-10 expression.

Secondly, monocytes from Africans displayed a clearly distinct, but mostly lower amino acid metabolism. Studies in rheumatoid arthritis patients have revealed that the pro-inflammatory phenotype of monocytes is dependent on an increased ability to take up amino acids [25], which makes it conceivable that the differences in amino acid metabolism between monocytes from the two populations contribute to their distinct inflammatory profiles. One notable exception to the overall lower levels of metabolism of amino acids in African monocytes was that of tyrosine, which was significantly increased. This was associated with increased concentrations of dopamine, of which tyrosine is the main precursor. Although dopamine is well-known for its neurological effects, it also modulates immune cell function, including that of myeloid cells. Dopamine has been shown to reduce TNF but increase IL-10 production following LPS stimulation of human macrophages [26], which warrants further study into exploring the contribution of dopamine in the differences we observed in inflammatory status of monocytes.

Finally, we found significantly elevated cytoplasmic ROS levels in monocytes from Africans compared to Europeans which we identified to be derived from increased NADPH oxidase activity. Furthermore, our data provide support for increased baseline PPP activity in African monocytes, presumably to provide NADPH to fuel enhanced NADPH-oxidase activity both prior and upon cellular activation. Most importantly, we demonstrated a critical role for this pathway in underpinning the heightened IL-10 production by African monocytes, as neutralizing cytoplasmic ROS either through blocking NADPH oxidase or PPP activity reduced LPS-induced IL-10 secretion selectively in African monocytes. ROS generated by NADPH oxidase is most well-known for playing an important role in host antimicrobial defence. In addition, induction of NADPH oxidase activity following activation of macrophages [27], monocytes [28] and HEK293 cells [29], has been shown to support pro-inflammatory cytokine responses by these cells. Our findings indicate that in Africans, monocytes increased NADPH-oxidase activity and ROS levels, already prior to stimulation, may have a different outcome and instead control IL-10 expression rather than pro-inflammatory cytokines upon subsequent activation. Indeed, pre-incubation of European monocytes with an SOD inhibitor significantly boosted superoxide accumulation in the cells and was sufficient to boost their IL-10 production

following LPS stimulation. This would be largely consistent with a study showing that chronic exposure to ROS in the context of kidney disease, resulted in increased IL-10 production by monocytes [30] and conversely monocytes from Chronic Granulomatous Disease patients, that have functional defects in NADPH oxidase, displayed reduced IL-10 production but not pro-inflammatory cytokines upon LPS stimulation [31].

We found that LPS-induced IL-10 mRNA expression was significantly decreased when NADPH oxidase was inhibited in African monocytes, indicating that ROS transcriptionally regulates IL-10 production. Yet, how ROS derived from NADPH oxidase promotes IL-10 mRNA expression in African monocytes remains to be addressed. Key regulators of IL-10 transcription are NF-kB subunits BCL3 and p50, CREB and transcription factors SP1 and 3 downstream of MAP kinase p38 [32-34] , and their activity or expression have been shown to be ROS sensitive [19, 20, 35-37]. Of note, in these studies primarily H_2O_2 has been shown to act on these targets, while in our hands superoxide but not H_2O_2 was capable of promoting IL-10 expression in monocytes. Further studies are required to determine if and how superoxide in monocytes promotes potentiates activity of one or more of these transcription factors to boost IL-10 mRNA expression, without significantly affecting expression of pro-inflammatory cytokines.

Our immunometabolic data extend previous studies that have documented differences in phenotype at baseline and functional responses following TLR stimulation of monocytes from individuals from Africa compared to Europe [3, 4]. The drivers behind these immunological differences – and as we find in this work - metabolic differences, are likely multifactorial. One such driver is the level of exposure to microorganisms and parasites which is much higher in African populations compared to those from Europe and known to have a major impact on the immune system and to promote immune-regulatory networks [38, 39]. Indeed, the immunological phenotype of the monocytes from Africans resembles that of tolerized monocytes that produce low pro-inflammatory and high anti-inflammatory cytokines upon LPS stimulation following low grade pre-exposure to LPS [40]. Moreover, metabolically, the altered redox balance, lower levels of OXPHOS, increased PPP [41] and NADPH oxidase activity [42] observed in African monocytes are strikingly similar to those reported in tolerized monocytes in the context of sepsis [43, 44], further supporting the notion that distinct microbial exposure is an important driver of the immunometabolic differences between monocytes from the Africans and Europeans.

Apart from differences in microbial exposure, differences in diet and lifestyle between the two groups may also influence the observed immunological differences [45]. For instance, recent work has shown that food-derived metabolites - highly abundant in rural-living individuals from Tanzania compared to those living in urban areas characterized by a western lifestyle - could account for an anti-inflammatory immune profile observed in those living in rural areas, rather than age, sex or genetic differences [45]. Finally, apart from these environmental factors, differences in genetics cannot be ruled out [46, 47]. This is illustrated by a study in which oxidative stress levels in cells from Afro-Americans, with genetic ties to West-Central Africa, and Caucasians from the same urban setting were compared [48]. Monocytes from Afro-Americans displayed increased levels of oxidative stress due to higher expression of NADPH oxidase, making it conceivable that differences in baseline NADPH oxidase expression in our two study groups may at least in part have a genetic basis.

In summary, we have uncovered a previously unappreciated role for metabolism in underpinning differences in anti-inflammatory IL-10 production of monocytes from two geographically distinct populations. Although future studies will be needed to validate our findings in more diverse cohorts, they provide potential new leads to modulate monocyte function in the context of combating infectious and chronic inflammatory diseases.

Materials and Methods

Sample collection

Peripheral blood mononuclear cells (PBMCs) were obtained from blood that healthy Dutch residents in the Netherlands donate voluntarily to LUMC Blood Bank. The donated material was processed and analysed anonymously. PBMCs from healthy Gabonese were collected as part of HOOKVAC trial (Clinicaltrials.gov ID: NCT02126462) prior to vaccine administration. Written informed consent was obtained from each participant (see **Table S1** for participants characteristics). The collected blood was processed and analysed anonymously.

Cell isolation

Venous blood of healthy volunteers living in Gabon (Africans) and in Netherlands (Europeans) were collected in heparin tubes followed by an isolation of PBMCs using 1.0772 Ficoll-Paque density gradient centrifugation. Isolated PBMCs were cryopreserved in 20% fetal bovine serum (FBS; lot number 45110321FBS

from SERANA) /10% dimethyl sulfoxide (DMSO)/ RPMI-1640 complete medium containing 1mM pyruvate, 2mM L-glutamine, 100U/ml penicillin, 10 µg/ml streptomycin (all from Sigma-Aldrich, CA, USA). Cryovials were stored overnight at -80°C in controlled-grade Mr. Frosty Freezing Container (Thermo Scientific, cat: 5100–0001) before transferring to liquid nitrogen for long term storage until analysis. PBMCs stored in Gabon were shipped to the Netherlands and monocytes were directly isolated from thawed PBMCs from both European and African using CD14 positive selection beads following manufacturer's instructions (Miltenyi Bioscience) with a purity of >95 % and a viability of >90 % and were directly cultured.

Extracellular flux analysis

Real time metabolic analysis on PBMCs or isolated monocytes was performed using XF96e Extracellular Flux analyser (Agilent) and analysed using Wave Desktop (Version 2.6, Agilent). Cells were counted and resuspended in pH 7.4 Seahorse media deprived from glucose and plated at $3x10^5$ of PBMCs or $1.5x10^5$ of monocytes. The XF cartridge was pre-hydrated and filled with the following reagents for sequential injection during the run : glucose (10 mM; port A; #G8644-100mL, Sigma), oligomycin (1 µM; port B; #11342, Cayman Chemical), fluoro-carbonyl cyanide phenylhydrazone (FCCP, 3 µM; port C; # C2920-10MG, Sigma), and finally, rotenone/antimycin A (1/1 µM; port D; #R8875-1G/#A8674-25MG, Sigma). Oxygen consumption rates (OCR) and extracellular acidification rates (ECAR) were recorded. Following metabolic parameters were calculated: Glycolysis rate = increase in ECAR in response to injection A. Glycolytic capacity = increase in ECAR in response to injection A and injection B. Baseline respiration = difference in OCR between readings following port A injection and readings after port D injection. Spare respiratory capacity = difference between baseline respiration and maximum mitochondrial respiration which is calculated based on the difference in OCR between readings following port C injection and readings after port A injection. ATP production = difference in OCR between readings following port A injection and readings after port B injection. At the end of the run XF culture plates supernatants were carefully discarded, cells were washed with PBS, lysed in 25 µL of a RIPA-like buffer (50 mM Tris-HCl [pH 7.4], 150 mM NaCl and 0.5% SDS) and the plate was stored at -20 degrees Celsius for later protein content quantification and normalization for cell input using bicinchoninic acid protein assay kit (BCA; #PIER23225, Pierce) according to the manufacturer's recommendations. A representative plot of extracellular flux analysis is shown in Figure 1A.

Cultures conditions and cytokine measurements

Monocytes were plated at $1x10^5$ cells per well and cultured for 24 hours in a total of 200µl of RPMI 1640 complete medium with TLR4 ligands and/or inhibitors. Ultrapure lipopolysaccharide (LPS; *Escherichia coli* 0111 B4 strain, #tlrl-3pelps, Invitrogen) was used at 100 ng/ml for 24 hours. Where indicated cells were pre-treated for 1 hour with the following compounds: 1 µM Oligomycin (Cayman Chemical, Ann Arbor, Michigan, United States), 1 µM rotenone/antimycin A (R/A; 1/1, Sigma-Aldrich), 10 mM 2-deoxyglucose (2DG; Sigma-Aldrich), 10 µM diphenyleiodonium chloride (DPI; Sigma-Aldrich), 100 µM 6-aminonicotinamide (6-AN; Sigma-Aldrich), 5 mM N-acetylcysteine amide (NAC; Sigma-Aldrich), 10 nM mitoquinone (MQ; Bio Vision), 10 µM 3-amino-1.2.4-triazole (3-AT; Sigma-Aldrich), 10 µM 2-methoxyestradiol (2-ME; Sigma-Aldrich), 1 Mm apocynin (APO; Sigma-Aldrich). These compounds were prepared in 100 µL of complete medium at their respective end concentration and added to the monocyte cultures 1h before LPS stimulation. Subsequently cells were used for different readouts.

Cytokine production

Stimulated cells were kept for a total of 24 hours in a 5% CO_2 and 37 degrees Celsius in the incubator. Supernatant were collected after 24 hours and concentrations of IL-10, IL-6, IL-1b and TNF were determined by ELISA (BD Biosciences) according to manufacturer's protocol.

Flow cytometry

Thawed PBMCs or isolated $CD14^+$ monocyte suspensions were directly stained with 50 µL of antibody cocktail (**Table S2**) for 30 min at 4°C, followed by LIVE/DEAD Fixable Aqua dead cell Stain Kit (Invitrogen, cat: L34957) for 15 min in the dark at room temperature (RT). Thereafter, cells were separately stained with 100 µL of following fluorescents metabolic dyes prepared in complete RPMI medium and put at 37°C in incubator for 30 min to assess superoxide levels with 10 µM of dihydroethidium (DHE; Sigma-Aldrich), total cellular ROS with 1 µM H2DCFDA (Invitrogen), mitochondrial ROS with 10 µM MitoSOX (Invitrogen), mitochondrial membrane potential with 20 nM of Tetramethyl rhodamine (TMRM , #T668, Invitrogen), mitochondrial mass with 1 µM Mitotracker Green (MitoSOX, #M7514, Invitrogen) and glucose uptake with 2-NBDG (10 µM, Invitrogen). Cells were acquired on BD FACS Canto II flow cytometer (BD Biosciences) and analysed using FlowJo V10 (Tree Star, San Carlos, CA).

For spectral flow cytometry measurements, thawed PBMCs were stained with LIVE/DEAD Zombie NIR for 15 min in the dark at room temperature (RT) following by a staining with a cocktail of surface markers antibodies (**Table S3**) for 15 min. Next, cells were fixed with 4% PFA (Thermo Scientific) for 15 min, permeabilised for 30 min and stained 30 min for a second time with 50 µL of metabolic antibodies cocktail freshly prepared in permeabilization buffer (**Table S4**). Cells were acquired in a 5-lasers Cytek Aurora cytometer together with calibration beads and analysed using FlowJo V10 (Tree Star, San Carlos, CA). Live $CD14^+$ monocytes were selected following gating strategy shown in **Figure S4** and mean fluorescence intensity (MFI) of each metabolic marker was recorded within the $CD14^+$ live monocytes.

RNA isolation + RT- qPCR

$CD14^+$ isolated monocytes were harvested after 24h LPS stimulation w/wo DPI and transferred in 1.5 Eppendorf vial. After 3 steps of centrifugation/ washing with PBS, the pellet was put in liquid nitrogen and stored at -80 degrees until the next day. RNA isolation was performed using NucleoSpin RNA kit (MACHERE-NAGEL kit, lot 1810/001) according to manufacturer instructions. Right after RNA isolation, cDNA synthesis was done by RT-qPCR. A total of 9 µL of RNA were combined with 11 µL of a mix (4 µL of 5x First-Strand buffer, 2 µL of 0.1 M DTT, 1 µL of RNaseOUT (40 U/uL), 1 µL hexamers/random primers (250 ng/uL), 2 µL dNTPs (6.25 mM each), 1 µL RT (M,MLV, 200u/uL), all from Invitrogen) following a program of 10 min. at 25°C, 50 min at 37°C and 15 min. at 70°C. Thereafter, RT-PCR was performed with 2 µL of cDNA obtained from each sample and mixed with 8 µL of a mix of H_2O, 2x SYBR Green Supermix (ThermoFisher), 20 µM of forward primer and reverse primer of IL-10 (Forward: AAGACCCAGACATCAAGGCG, Reverse: CAGGGAAGAAATCGATGACAGC from Eurofins Genomics) or the control Beta-2-M (B2M, Forward: GCCTGCCGTGTGAACCAT, Reverse: GGTTGACTGAAGTTAGCAAGCA from Eurogentec). For RT-PCR, all samples were plated in duplicate and mean Ct values was recorded together with their standard deviation for IL10 and B2M. The differential mRNA gene expression for each sample was calculated by Delta Delta Ct (ΔΔCt) relative to the control B2M and set to 2 ($2^{-\Delta\Delta Ct}$). $\Delta Ct_{(sample\ A)} = Mean\ Ct_{IL10(sample\ A)} - Ct_{B2M(sample\ A)}$, $\Delta\Delta Ct_{(sample\ A)} = mean\ Ct_A - \Delta Ct_{(sample\ A)}$.

NADPH quantification

NADPH levels were quantified using $1x10^6$ isolated $CD14^+$ monocytes as input using NADPH colorimetric assay kit (ab186031; abcam) following manufacturer's recommendations.

G6PDH activity

Glucose-6 phosphate dehydrogenase (G6PDH) activity was measured using $5x10^5$ isolated $CD14^+$ monocytes as input using the G6PDH colorimetric assay kit (catalog number MAK015; Sigma-Aldrich) according to the manufacturer's instructions.

Metabolite extraction and LC-MS Metabolomics

Monocyte lysates were extracted at minimum of $5x10^5$ cells in 700 µL of a pre-heated 70°C extraction solvent (70% ethanol: 7ml EtOH,3ml HPLC-grade water) after washing twice the monocyte suspension with a solution containing ammonium carbonate (75mM, Sigma-Aldrich) and HPLC-grade water, adjusted to pH 7.3-7.5 and kept at 37°C in an incubator. Samples were centrifugated at 14,000 rpm for 10 min at 4°C and 500 µL of the extract supernatant from each centrifugated sample were transferred to a pre-chilled microtube without disturbing the pellet material. Extract supernatants were stored at -80°C until shipped to General Metabolics LLC in Boston-USA for quantitative metabolomic analysis. Polar metabolites were analysed according to General Metabolic' high-throughput, non-targeted metabolomics platform in negative ion mode [49]. Each sample was injected twice. Mean ion intensity (m/z) data for each annotated metabolite was provided. A total of 817 metabolites were annotated. Metabolites with above 200 ion m/z were drug-related metabolites and were not considered for the analysis. From the remaining ones (n=315), only 277 metabolites that have an HMDB identification (HMDB ID) were considered for differential analysis.

Differential analysis

To analyse the differential abundance of each metabolite between monocytes from Africans and Europeans, we used *limma* R/Bioconductor package on log2-transformed mean ion intensity data using the R statistical software version 4.0.2. For the differential metabolite abundance analysis, false discovery rate (FDR) correction was applied and metabolites with FDR below 0.05 level were considered significant. Visualisation of the differential analysis was performed using volcano plot and heatmap, which were generated using ggplot2 and ComplexHeatmap R package, respectively.

Pathway enrichment analysis

Metabolite with HMDB identification (HMDB ID) that are upregulated in Africans and in Europeans were loaded in MetaboAnalyst 5.0 (https://genap.metaboanalyst.ca/MetaboAnalyst) for pathway analysis. In addition, the results table of the differential analysis, containing p-value (FDR = adjusted p-value) and log2 fold change (log2FC), was loaded in https://artyomovlab.wustl.edu/shiny/gatom/ to perform pathway analysis (network topology). The network summary built was generated as the .xgmml's file. This network file was then imported to Cytoscape 3.9.1 for styling and visualisation.

Data availability

All data are available in the main text or in the supplementary materials.

Study approval

The HOOKVAC trial was approved by the national ethical committee of Gabon (#0033/2014/SG/CNE) and done under an investigation new drug application (IND#016184) to the US Food and Drug administration. Written informed consent was obtained from each participant. Participants found to be infected with parasitic helminths was treated two weeks prior to vaccination (Table S1). Participants of the trial were healthy and free of HIV, hepatitis B or malaria parasites before vaccination. The trial followed the principle of the Declaration of Helsinki, Good Clinical Practice, and Good Clinical and Laboratory Practice.

Statistical analysis

Data were analysed for statistical significance using GraphPad Prism 9.3 statistical software (GraphPad Software, La Jolla, CA, USA). Comparison between Africans and Europeans for OCR , ECAR, cytokines, and cytometry data were performed using the paired or unpaired Student's t-test. All statistically significant comparisons are annotated using asterisks * $P < 0.05$, ** $P < 0.01$, *** $P < 0.001$. For significance between Africans and Europeans we used unpaired student's T test and for significance within each group, we used paired student's T test.

Acknowledgments

This work was funded by an LUMC fellowship (B.E.) and supported by NIH grant (U01A165745) (M.Y.). The funders had no role in study design, data collection and analysis, decision to publish, or preparation of the manuscript.

Author contributions

Conceptualization: M.E.B.O., B.E., M.Y.; **Methodology:** M.E.B.O., B.E., M.Y.; **Software**: M.E.B.O., M.D.M., B.E.; **Formal analysis:** M.E.B.O., B.E., M.Y.; **Investigation:** M.E.B.O., Y.D.M., A.A.A.; **Data curation:** M.E.B.O.., B.E.; **Visualization:** M.E.B.O., M.D.M., B.E., M.Y.; **Supervision:** B.E., M.Y.; **Validation:** M.E.B.O., B..E; **Project administration**: B.E., M.Y.; **Writing—original draft preparation:** M.E.B.O.; **Writing—review and editing:** M.E.B.O., Y.D.M., M.D.M., G.H., S.A., A.A.A., P.G.K., T.W.K., B.E., M.Y.

Conflicts of interest

The authors declare no conflict of interest.

REFERENCES

1. Brodin P, Davis MM. Human immune system variation. Nat Rev Immunol. 2017;17(1):21-9.
2. van Dorst M, Pyuza JJ, Nkurunungi G, Kullaya VI, Smits HH, Hogendoorn PCW, et al. Immunological factors linked to geographical variation in vaccine responses. Nat Rev Immunol. 2023.
3. Appleby LJ, Nausch N, Midzi N, Mduluza T, Allen JE, Mutapi F. Sources of heterogeneity in human monocyte subsets. Immunol Lett. 2013;152(1):32-41.
4. Quach H, Rotival M, Pothlichet J, Loh YE, Dannemann M, Zidane N, et al. Genetic Adaptation and Neandertal Admixture Shaped the Immune System of Human Populations. Cell. 2016;167(3):643-56 e17.
5. O'Neill MB, Quach H, Pothlichet J, Aquino Y, Bisiaux A, Zidane N, et al. Single-Cell and Bulk RNA-Sequencing Reveal Differences in Monocyte Susceptibility to Influenza A Virus Infection Between Africans and Europeans. Front Immunol. 2021;12:768189.
6. Austermann J, Roth J, Barczyk-Kahlert K. The Good and the Bad: Monocytes' and Macrophages' Diverse Functions in Inflammation. Cells. 2022;11(12).
7. Yang J, Zhang L, Yu C, Yang X-F, Wang H. Monocyte and macrophage differentiation: circulation inflammatory monocyte as biomarker for inflammatory diseases. Biomarker Research. 2014;2(1):1.
8. Shi C, Pamer EG. Monocyte recruitment during infection and inflammation. Nature Reviews Immunology. 2011;11(11):762-74.
9. Lachmandas E, Boutens L, Ratter JM, Hijmans A, Hooiveld GJ, Joosten LA, et al. Microbial stimulation of different Toll-like receptor signalling pathways induces diverse metabolic programmes in human monocytes. Nat Microbiol. 2016;2:16246.
10. Zhang B, Moorlag SJ, Dominguez-Andres J, Bulut O, Kilic G, Liu Z, et al. Single-cell RNA sequencing reveals induction of distinct trained-immunity programs in human monocytes. J Clin Invest. 2022;132(7).
11. Zhu X, Meyers A, Long D, Ingram B, Liu T, Yoza BK, et al. Frontline Science: Monocytes sequentially rewire metabolism and bioenergetics during an acute inflammatory response. J Leukoc Biol. 2019;105(2):215-28.
12. Yamada KJ, Heim CE, Xi X, Attri KS, Wang D, Zhang W, et al. Monocyte metabolic reprogramming promotes pro-inflammatory activity and Staphylococcus aureus biofilm clearance. PLoS Pathog. 2020;16(3):e1008354.
13. de Jong SE, van Unen V, Manurung MD, Stam KA, Goeman JJ, Jochems SP, et al. Systems analysis and controlled malaria infection in Europeans and Africans elucidate naturally acquired immunity. Nat Immunol. 2021;22(5):654-65.
14. Ahl PJ, Hopkins RA, Xiang WW, Au B, Kaliaperumal N, Fairhurst AM, Connolly JE. Met-Flow, a strategy for single-cell metabolic analysis highlights dynamic changes in immune subpopulations. Commun Biol. 2020;3(1):305.
15. Pelgrom LR, Patente TA, Otto F, Nouwen LV, Ozir-Fazalalikhan A, van der Ham AJ, et al. mTORC1 signaling in antigen-presenting cells of the skin restrains CD8(+) T cell priming. Cell Rep. 2022;40(1):111032.
16. Mills EL, Kelly B, Logan A, Costa ASH, Varma M, Bryant CE, et al. Succinate Dehydrogenase Supports Metabolic Repurposing of Mitochondria to Drive Inflammatory Macrophages. Cell. 2016;167(2):457-70 e13.
17. Canton M, Sanchez-Rodriguez R, Spera I, Venegas FC, Favia M, Viola A, Castegna A. Reactive Oxygen Species in Macrophages: Sources and Targets. Front Immunol. 2021;12:734229.
18. Britt EC, Lika J, Giese MA, Schoen TJ, Seim GL, Huang Z, et al. Switching to the cyclic pentose phosphate pathway powers the oxidative burst in activated neutrophils. Nat Metab. 2022;4(3):389-403.
19. Ndengele MM, Muscoli C, Wang ZQ, Doyle TM, Matuschak GM, Salvemini D. Superoxide potentiates NF-kappaB activation and modulates endotoxin-induced cytokine production in alveolar macrophages. Shock. 2005;23(2):186-93.

20. Gloire G, Legrand-Poels S, Piette J. NF-kappaB activation by reactive oxygen species: fifteen years later. Biochem Pharmacol. 2006;72(11):1493-505.

21. Buttgereit F, Brand MD. A hierarchy of ATP-consuming processes in mammalian cells. Biochem J. 1995;312 (Pt 1)(Pt 1):163-7.

22. Tannahill GM, Curtis AM, Adamik J, Palsson-McDermott EM, McGettrick AF, Goel G, et al. Succinate is an inflammatory signal that induces IL-1beta through HIF-1alpha. Nature. 2013;496(7444):238-42.

23. Cheng MX, Cao D, Chen Y, Li JZ, Tu B, Gong JP. alpha-ketoglutarate attenuates ischemia-reperfusion injury of liver graft in rats. Biomed Pharmacother. 2019;111:1141-6.

24. Liu PS, Wang H, Li X, Chao T, Teav T, Christen S, et al. alpha-ketoglutarate orchestrates macrophage activation through metabolic and epigenetic reprogramming. Nat Immunol. 2017;18(9):985-94.

25. Yoon BR, Oh YJ, Kang SW, Lee EB, Lee WW. Role of SLC7A5 in Metabolic Reprogramming of Human Monocyte/Macrophage Immune Responses. Front Immunol. 2018;9:53.

26. Gaskill PJ, Carvallo L, Eugenin EA, Berman JW. Characterization and function of the human macrophage dopaminergic system: implications for CNS disease and drug abuse. J Neuroinflammation. 2012;9:203.

27. Erlich JR, To EE, Luong R, Liong F, Liong S, Oseghale O, et al. Glycolysis and the Pentose Phosphate Pathway Promote LPS-Induced NOX2 Oxidase- and IFN-beta-Dependent Inflammation in Macrophages. Antioxidants (Basel). 2022;11(8).

28. Ruggeri Barbaro N, Van Beusecum J, Xiao L, do Carmo L, Pitzer A, Loperena R, et al. Sodium activates human monocytes via the NADPH oxidase and isolevuglandin formation. Cardiovasc Res. 2021;117(5):1358-71.

29. Park HS, Jung HY, Park EY, Kim J, Lee WJ, Bae YS. Cutting edge: direct interaction of TLR4 with NAD(P)H oxidase 4 isozyme is essential for lipopolysaccharide-induced production of reactive oxygen species and activation of NF-kappa B. J Immunol. 2004;173(6):3589-93.

30. Sardenberg C, Suassuna P, Watanabe R, Cruz Andreoli MC, Aparecida Dalboni M, Faria Seabra V, et al. Balance between cytokine production by peripheral blood mononuclear cells and reactive oxygen species production by monocytes in patients with chronic kidney disease. Ren Fail. 2004;26(6):673-81.

31. Gazendam RP, van de Geer A, van Hamme JL, Helgers L, Rohr J, Chrabieh M, et al. Proinflammatory cytokine response toward fungi but not bacteria in chronic granulomatous disease. J Allergy Clin Immunol. 2016;138(3):928-30 e4.

32. Chanteux H, Guisset AC, Pilette C, Sibille Y. LPS induces IL-10 production by human alveolar macrophages via MAPKinases- and Sp1-dependent mechanisms. Respir Res. 2007;8(1):71.

33. Tone M, Powell MJ, Tone Y, Thompson SA, Waldmann H. IL-10 gene expression is controlled by the transcription factors Sp1 and Sp3. J Immunol. 2000;165(1):286-91.

34. Wen AY, Sakamoto KM, Miller LS. The role of the transcription factor CREB in immune function. J Immunol. 2010;185(11):6413-9.

35. Ryu H, Lee J, Zaman K, Kubilis J, Ferrante RJ, Ross BD, et al. Sp1 and Sp3 are oxidative stress-inducible, antideath transcription factors in cortical neurons. J Neurosci. 2003;23(9):3597-606.

36. Kumashiro N, Tamura Y, Uchida T, Ogihara T, Fujitani Y, Hirose T, et al. Impact of oxidative stress and peroxisome proliferator-activated receptor gamma coactivator-1alpha in hepatic insulin resistance. Diabetes. 2008;57(8):2083-91.

37. Ichiki T, Tokunou T, Fukuyama K, Iino N, Masuda S, Takeshita A. Cyclic AMP response element-binding protein mediates reactive oxygen species-induced c-fos expression. Hypertension. 2003;42(2):177-83.

38. Yazdanbakhsh M, Kremsner PG, van Ree R. Allergy, parasites, and the hygiene hypothesis. Science. 2002;296(5567):490-4.

39. Pfefferle PI, Keber CU, Cohen RM, Garn H. The Hygiene Hypothesis - Learning From but Not Living in the Past. Front Immunol. 2021;12:635935.

40. Frankenberger M, Pechumer H, Ziegler-Heitbrock HW. Interleukin-10 is upregulated in LPS tolerance. J Inflamm. 1995;45(1):56-63.

41. Ferreira BL, Sousa MB, Leite GGF, Brunialti MKC, Nishiduka ES, Tashima AK, et al. Glucose metabolism is upregulated in the mononuclear cell proteome during sepsis and supports endotoxin-tolerant cell function. Front Immunol. 2022;13:1051514.

42. Santos SS, Carmo AM, Brunialti MK, Machado FR, Azevedo LC, Assuncao M, et al. Modulation of monocytes in septic patients: preserved phagocytic activity, increased ROS and NO generation, and decreased production of inflammatory cytokines. Intensive Care Med Exp. 2016;4(1):5.

43. Cheng SC, Scicluna BP, Arts RJ, Gresnigt MS, Lachmandas E, Giamarellos-Bourboulis EJ, et al. Broad defects in the energy metabolism of leukocytes underlie immunoparalysis in sepsis. Nat Immunol. 2016;17(4):406-13.

44. Widdrington JD, Gomez-Duran A, Pyle A, Ruchaud-Sparagano MH, Scott J, Baudouin SV, et al. Exposure of Monocytic Cells to Lipopolysaccharide Induces Coordinated Endotoxin Tolerance, Mitochondrial Biogenesis, Mitophagy, and Antioxidant Defenses. Front Immunol. 2018;9:2217.

45. Temba GS, Kullaya V, Pecht T, Mmbaga BT, Aschenbrenner AC, Ulas T, et al. Urban living in healthy Tanzanians is associated with an inflammatory status driven by dietary and metabolic changes. Nat Immunol. 2021;22(3):287-300.

46. Dai Z, Ramesh V, Locasale JW. The evolving metabolic landscape of chromatin biology and epigenetics. Nature Reviews Genetics. 2020;21(12):737-53.

47. Cavalli G, Heard E. Advances in epigenetics link genetics to the environment and disease. Nature. 2019;571(7766):489-99.

48. Smolen KK, Cai B, Fortuno ESR, Gelinas L, Larsen M, Speert DP, et al. Single-cell analysis of innate cytokine responses to pattern recognition receptor stimulation in children across four continents. J Immunol. 2014;193(6):3003-12.

49. Fuhrer T, Heer D, Begemann B, Zamboni N. High-throughput, accurate mass metabolome profiling of cellular extracts by flow injection-time-of-flight mass spectrometry. Anal Chem. 2011;83(18):7074-80.

Supplementary documents

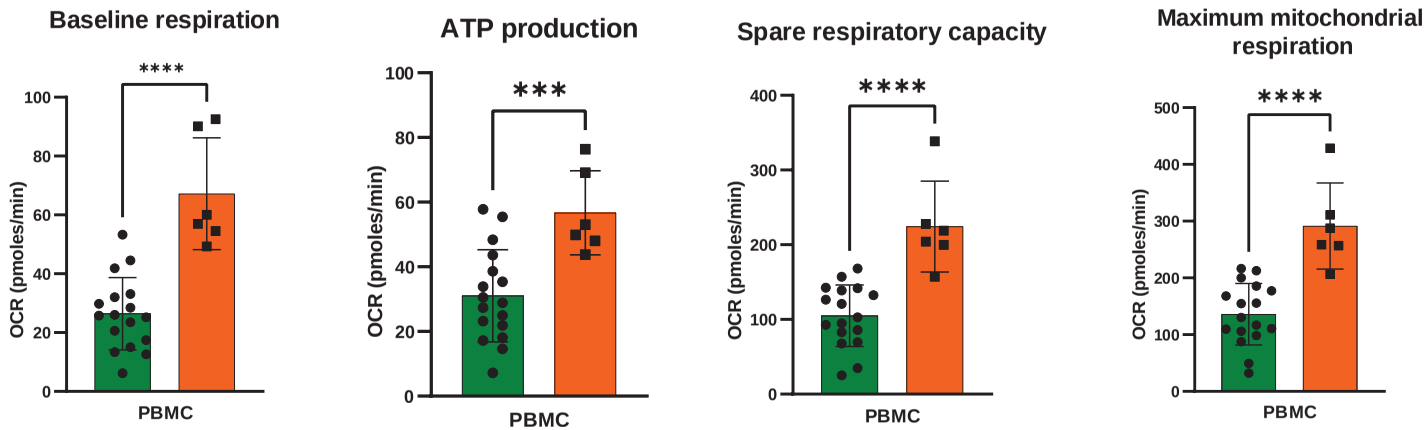

Figure S1. Oxygen consumption rate (OCR) linked to baseline respiration, ATP production, spare respiratory capacity and maximum mitochondrial respiration were measured on live PBMCs from Africans (green) and Europeans(orange). Bars represented mean ± SD; each dot represents one individual. *, P < 0.05, **,P<0.01, ***P<0.001, ****P<0.0001 for significant differences between Europeans and Africans based on unpaired Student's T test.

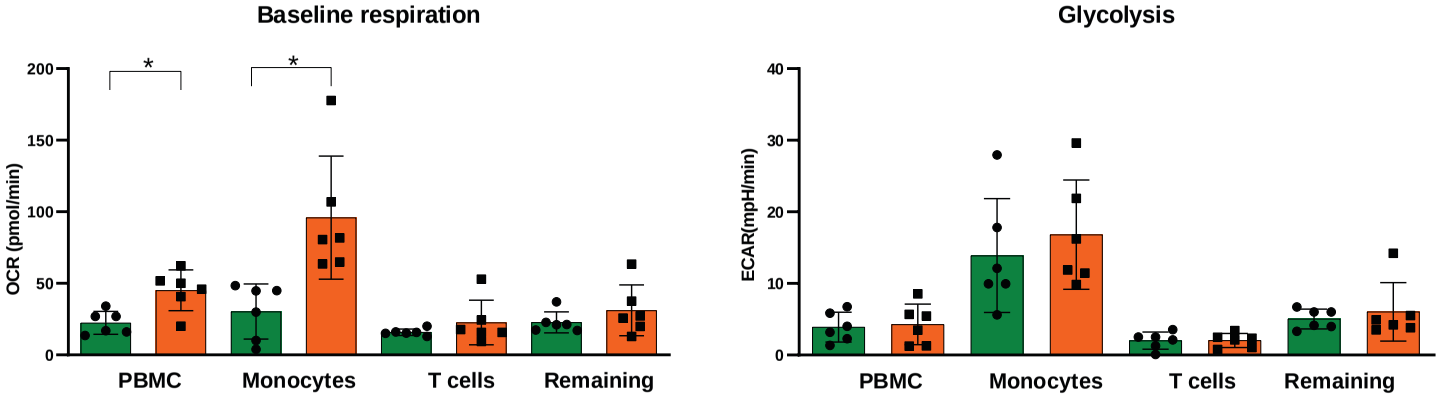

Figure S2. Oxygen consumption rate (OCR) linked to baseline respiration and extracellular acidification rate linked to glycolysis were measured on isolated $CD14^+$ monocytes, $CD4^+$ T cells and the remaining cells referred as "Remaining" of their respective PBMCs from Africans (green) and Europeans (orange). Bars represented mean ± SD; each dot represents one individual. *, $P < 0.05$, for significant difference between Africans and Europeans based on unpaired Student's T test.

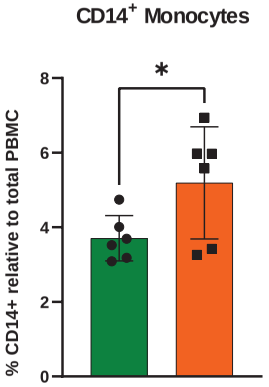

Figure S3. Percentage of CD14⁺ monocytes relative to total PBMCs of Africans (green) and Europeans (orange). Bars represented mean ± SD; each dot represents one individual. *, P < 0.05, for significant difference between Africans and Europeans based on unpaired Student's T test.

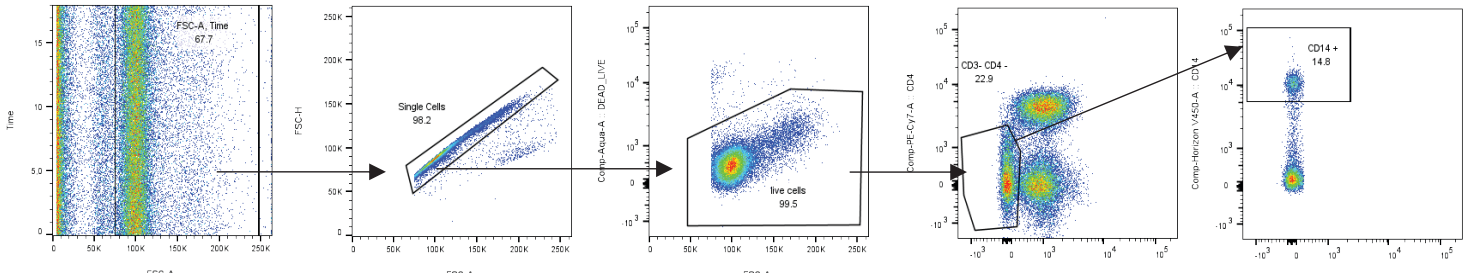

Figure S4. CD14⁺ monocytes gating strategy. Flow cytometry gating strategy to select CD14⁺ monocytes for one representative sample. Cells were first gated on time and then on forward scatter (FSC)-H to select singlets. Thereafter, live cells were selected from the gate on viability dye. The CD14⁺ monocytes were lastly selected after excluding CD3⁺ and CD4⁺ cells from total PBMCs.

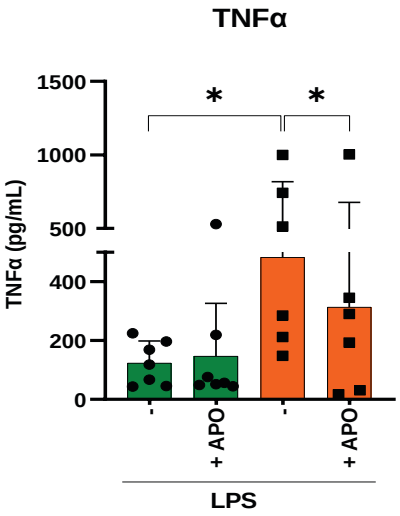

Figure S5. TNFα production by monocytes of Africans (green) and Europeans (orange) after LPS stimulation in presence or absence of apocynin (APO) as determined by ELISA in culture supernatants. Bars represent mean mean ± SD; each dot represents one individual. *, P < 0.05, for significant difference between Africans and Europeans and within Europeans based on unpaired and paired Student's T test respectively.

Table S1: Characteristics of study participants

Characteristics	Gabonese	Dutch
number	32	17
Age, years (Mean, SD)	25.5 (8.7)	32.9 (12.1)
Male, n (%)	24 (75%)	4 (23.5%)
Infectious status of HOOKVAC Gabonese participants prior the vaccination		
Schistosoma haematobium, n (%)	9 (28.1%)	
Ascaris lombricoides, n (%)	2 (6.2 %)	
Trichuris trichiura, n (%)	5 (15.6 %)	
Necator americanus, n (%)	4 (12.5 %)	
Helminth infected (mono- or poly-), n (%)	20 (62.5 %)	

Table S2. List of antibodies used for PBMCs in flow cytometry.

Antibodies	Catalogue number	clone	supplier	Dilution
CD56 PerCP ef710	46-0567-42	CMSSB	eBioscience	800
CD4 PE-cy7	557852	SK3	BD	150
CD3 APC –eF780	47-0038-42	UCHT1	Invitrogen	800
CD14 HV 450	560349	MFP10	BD	800
LIVE/DEAD Fixable Aqua Dead Cell Stain Kit	L34957		Thermo Fisher	400
FcR inhibitor	14-9161-73		Invitrogen	100

Table S3: List of surface antibodies used for spectral cytometry.

Antibodies	Label	Catalogue number	Clone	Supplier	Dilution
CD4	SB550	344655	SK3	Biolegend	50
CD3	BUV496	612941	CMSSB	eBioscience	50
CD14	BV570	301831	M5E2	Biolegend	100
HLA-DR	APCFire810	307673	L243	Biolegend	100
CD56	BUV737	612767	NCAM16.2	BD	200
CD16	BUV563	748851	3G8	BD	400
CD19	BV750	302262	HIB19	Biolegend	200
Live/dead	Zombie NIR Fixable Viability Kit	423106		Biolegend	2000
Brillant stain Buffer Plus		566385		BD Horizon	10
FcR blocker		14-9161-73		Invitrogen	100

Table S4: List of metabolic antibodies used for spectral cytometry.

Antibodies	Label	Catalogue number	Supplier	Dilution
Glucose transporter 1 (GLUT1)	DL405	ab252403/ab201798	Abcam	200
Pyruvate Kinase M (PKM)	PE	ab206129/ab102918	Abcam	200
Cytochrome C (Cyt C)	PE cy7	ab237966/ab102903	Abcam	200
Carnitine palmitoyl transferase 1A (CPT1A)	PE-Cy5	ab235841/ab102893	Abcam	200
Succinate Dehydrogenase A (SDHA)	AF647	ab240098/ab195884	Abcam	200
Brillant stain Buffer Plus		566385	BD Horizon	10
FcR blocker		14-9161-73	Invitrogen	100
mono blocker		426103	Biolegend	20